Potent *In vitro* and *In vivo* Activity of an Fc-Engineered Anti-CD19 Monoclonal Antibody against Lymphoma and Leukemia

Holly M. Horton,[1] Matthew J. Bernett,[1] Erik Pong,[1] Matthias Peipp,[2] Sher Karki,[1] Seung Y. Chu,[1] John O. Richards,[1] Igor Vostiar,[1] Patrick F. Joyce,[1] Roland Repp,[2] John R. Desjarlais,[1] and Eugene A. Zhukovsky[1]

[1]Xencor, Inc., Monrovia, California and [2]Section of Stem Cell Transplantation and Immunotherapy, Christian-Albrechts-University, Kiel, Germany

Abstract

CD19 is a pan B-cell surface receptor expressed from pro–B-cell development until its down-regulation during terminal differentiation into plasma cells. CD19 represents an attractive immunotherapy target for cancers of lymphoid origin due to its high expression levels on the vast majority of non–Hodgkin's lymphomas and some leukemias. A humanized anti-CD19 antibody with an engineered Fc domain (XmAb5574) was generated to increase binding to Fcγ receptors on immune cells and thus increase Fc-mediated effector functions. *In vitro*, XmAb5574 enhanced antibody-dependent cell-mediated cytotoxicity 100-fold to 1,000-fold relative to an anti-CD19 IgG1 analogue against a broad range of B-lymphoma and leukemia cell lines. Furthermore, XmAb5574 conferred antibody-dependent cell-mediated cytotoxicity against patient-derived acute lymphoblastic leukemia and mantle cell lymphoma cells, whereas the IgG1 analogue was inactive. XmAb5574 also increased antibody-dependent cellular phagocytosis and apoptosis. *In vivo*, XmAb5574 significantly inhibited lymphoma growth in prophylactic and established mouse xenograft models, and showed more potent antitumor activity than its IgG1 analogue. Comparisons with a variant incapable of Fcγ receptor binding showed that engagement of these receptors is critical for optimal antitumor efficacy. These results suggest that XmAb5574 exhibits potent tumor cytotoxicity via direct and indirect effector functions and thus warrants clinical evaluation as an immunotherapeutic for CD19$^+$ hematologic malignancies. [Cancer Res 2008;68(19):8049–57]

Introduction

CD19 is a 95-kDa transmembrane glycoprotein of the immunoglobulin superfamily containing two extracellular immunoglobulin-like domains and an extensive cytoplasmic tail (1). It is B-lineage–specific and functions as a positive regulator of B-cell receptor signaling in conjunction with CD21 and CD81. CD19 is an attractive target for cancers of lymphoid origin due to its high expression in most non–Hodgkin's lymphomas (NHL) and many leukemias, including acute lymphoblastic leukemia (ALL), chronic lymphocytic leukemia (CLL), and hairy cell leukemia (HCL; refs. 2, 3). NHL is the most prevalent of all lymphoproliferative diseases, and 85% of NHLs are classified as B-cell disorders (4). In the last decade, many B-NHLs and some B-cell leukemias have been successfully treated by combining chemotherapy with rituximab, a chimeric anti-CD20 antibody, demonstrating the utility of immunotherapies in B-cell diseases. CD19 cell surface expression is lower relative to CD20, but it begins earlier and persists longer through B-cell maturation (1). Consequently, the spectrum of lymphoid malignancies expressing CD19 is broader (2). Moreover, although the chemotherapy-rituximab regimen has led to major improvements in response rates and progression-free survival, some B-cell tumors either lack CD20 expression or lose it during the course of rituximab treatment (5, 6). Consequently, some patients do not respond to rituximab, and many of those that respond will relapse (7). Thus, anti-CD19 antibodies may be efficacious against early B-cell malignancies such as ALL or other CD20$^-$ tumors, which are not amenable to treatment with rituximab, and as salvage regimens for patients failing rituximab.

CD19 has been a focus of immunotherapy development for over 20 years, and several CD19-specific antibodies have been evaluated for the treatment of B-lineage malignancies *in vitro*, in mouse models, and in clinical trials. These have included unmodified anti-CD19 antibodies (8, 9), antibody-drug conjugates (10–12), and bispecific antibodies targeting CD19 and CD3 (13) or CD16 (14) to engage cytotoxic lymphocyte effector functions. Although early clinical studies with murine unconjugated CD19 antibodies showed safety and responses in individual patients, these responses were not durable (15). However, recent phase I trials with bispecific antibodies have yielded encouraging results (16). These clinical studies as well as trials with anti-CD19 immunoconjugates have validated CD19 as a target for B-cell malignancies, and the results with bispecific antibodies indicate that enhancing the engagement of immune effector functions may improve therapeutic efficacy.

Immune effector functions which have been shown to contribute to antibody-mediated cytotoxicity include antibody-dependent cell-mediated cytotoxicity (ADCC), antibody-dependent cell-mediated phagocytosis (ADCP), and complement-dependent cytotoxicity (CDC). Cytotoxicity may also be mediated via antiproliferative effects. The mechanism of antibody modulation of tumor cell proliferation is poorly understood. However, advances in understanding the interactions of antibodies with Fcγ receptors (FcγR) on immune effector cells have allowed the engineering of antibodies with significantly improved effector function (17). Protein engineering of the Fc domain has been used to improve binding to FcγRs (18–21), and antibodies with up to 100-fold greater affinity for FcγRIIIa relative to native IgG1 have been generated, leading to significant improvements in ADCC (19). These results, in conjunction with studies in mouse models demonstrating that anti-CD19 antibodies deplete B cells in an FcγR-dependent fashion (9, 22), suggested that engineering an anti-CD19 antibody to increase FcγR binding could enhance its cytotoxic potential.

Requests for reprints: Eugene A. Zhukovsky, Xencor, Inc., 111 West Lemon Avenue, Monrovia, CA 91016. Phone: 626-737-8183; Fax: 626-305-0350; E-mail: ezhukovsky@xencor.com.

doi:10.1158/0008-5472.CAN-08-2268

Here, we describe the characterization of XmAb5574, a humanized anti-CD19 antibody with increased FcγR binding that has highly enhanced ADCC against multiple NHL and leukemia cell lines and primary ALL and mantle cell lymphoma (MCL) tumor cells. XmAb5574 also increases ADCP and antiproliferative activity, and inhibits lymphoma growth in Ramos and Raji mouse xenograft models. Therefore, XmAb5574 may represent a promising next-generation immunotherapeutic for B-cell malignancies.

Materials and Methods

Production of antibodies, FcγRs, and FcγRIIIa–glutathione-*S*-transferase. Variable region genes for mouse anti-CD19 antibody (clone 4G7; ref. 23) or anti-CD22 antibody (RFB4) were ligated into the expression vector pcDNA3.1Zeo (Invitrogen) comprising the human light chain κ and heavy chain constant regions to produce constructs for the corresponding chimeric antibodies. To generate XmAb5574, the Fv of 4G7 was humanized (24) and affinity-matured using library design automation,[3] and substitutions S239D/I332E were introduced into the human Fc domain using standard molecular biology techniques. The IgG1 analogue of XmAb5574 (anti-CD19 IgG1) and the anti-CD19 Fc-knockout (anti-CD19 Fc-KO) both used an Fv identical to that of XmAb5574, but for the analogue, the Fc was wild-type IgG1, and for the anti-CD19 Fc-KO, two substitutions (G236R/L328R) were introduced to remove FcγR interactions. The XmAb isotype control was constructed in the same way as XmAb5574 (containing the S239D/I332E mutations), except that the Fv for anti–respiratory syncytial virus (25) was used. Light and heavy chain constructs were cotransfected into 293E cells (National Research Council Canada-Biotechnology Research Institute), and antibodies were purified using protein A chromatography (GE Healthcare). Rituximab was obtained from RxUSA. Human and mouse Fc receptors for binding studies were obtained from R&D Systems or constructed internally, all with 6× His tags. FcγRIIIa-158V glutathione-*S*-transferase (GST) was cloned into a pCDNA3.1 vector, expressed in 293T cells (Invitrogen), and purified using nickel affinity chromatography.

Cell lines, donors, and patients. SU-DHL-6, Bonna-12, BV-173, SUP-B15, RS4;11, Ramos, and Namalwa cell lines were obtained from DSMZ (German Collection of Microorganisms and Cell Lines). Raji was obtained from American Type Culture Collection, and WaC3CD5 was provided by John Byrd (Ohio State University, Columbus, OH).

Peripheral blood samples were obtained from healthy volunteers or from male patients with ALL or MCL expressing high levels of CD19. All protocols were performed with written informed consent in accordance with the Declaration of Helsinki and were approved by the Ethical Committee of the Christian-Albrechts-University, Campus Kiel. The percentages of tumor cells and CD19 expressions were determined using directly labeled antibodies and analyzed by fluorescence-activated cell sorting on a Cytomics FC500 (Beckman Coulter).

Internalization. XmAb5574, rituximab, or chimeric RFB4 antibodies were labeled with europium using the DELFIA europium-N1 ITC chelate kit (Perkin-Elmer). Raji cells were resuspended at 10^6 cells/mL in growth medium (RPMI 1640 medium supplemented with 10% fetal bovine serum; FBS) containing 4 nmol/L of europium-labeled antibody and incubated with mixing for 1 h at 4°C. Cells were washed in ice-cold PBS, resuspended in growth medium, and dispensed into 12-well plates. At the indicated times, samples were split into two aliquots; each was centrifuged and supernatant was saved. Pellets were washed in PBS to determine total cell-associated signal (surface bound plus internalized antibody) or in 0.5% acetic acid/125 mmol/L NaCl to determine internalized antibody, resuspended in PBS, mixed with DELFIA Enhancement Solution, and incubated for 1 h. Europium fluorescence was measured in 96-well plates using EnVision 2012 (Perkin-Elmer).

Fc receptor binding. Surface plasmon resonance (SPR) measurements were performed using a Biacore 3000 (Biacore). Antibodies were captured onto an immobilized protein A/G (Thermo Scientific) CM5 biosensor chip (Biacore) generated using a standard primary amine coupling protocol. All measurements were performed in 10 mmol/L Hepes/150 mmol/L NaCl/3 mmol/L EDTA/0.005% polysorbate-20; glycine buffer was used for protein A/G surface regeneration. Antibodies were immobilized on the protein A/G surface for 5 min at 1 μL/min. Fc receptors were injected over the antibody-bound surface for 2 min at 20 μL/min followed by a 2 to 3 min dissociation phase. Data were fit to a 1:1 binding model (Langmuir) using BIAevaluation software (Biacore). Binding curves corresponding to six FcγR concentration series were fitted individually. Kinetic variables were used to calculate the affinity constant (K_a).

CD19 binding. CD19 binding K_as were determined by employing a Raji cell–based competitive binding assay. Cells were centrifuged, washed with dilution buffer (PBS containing 0.1% bovine serum albumin and 0.1 mg/mL non–B-cell reactive IgG), and diluted to a density of 0.5×10^6 cells/mL. XmAb5574 was labeled with Alexa Fluor 647 protein labeling kit (Invitrogen) and the K_a was measured using a direct binding assay. Serial dilutions of labeled XmAb5574 were incubated with cells, washed, and analyzed on a FACSCanto II. Data were analyzed with a 1:1 binding model. K_as of unlabeled anti-CD19 antibodies were determined in a competition binding assay. Serial dilutions of antibodies (starting at 7.5 μg/mL) were mixed with 75 ng/mL of fluorescently labeled XmAb5574, incubated with cells for 1 h, and analyzed on a FACSCanto II. Data were analyzed by the simplified binding model of Cheng and Prusoff (26).

Cell lines ADCC: fluorescence. Isolated interleukin 2 (IL-2)–activated natural killer (NK) cells were used as effector cells. Human peripheral blood mononuclear cells (PBMC) were purified from leukopacks using a Ficoll gradient and NK cells were isolated using NK Cell Isolation kit II (Miltenyi Biotec). NK cells were incubated in RPMI 1640 medium supplemented with 10% FBS and 10 ng/mL of IL-2 at 37°C overnight. Tumor cell line target cells were seeded into 96-well plates at 10,000 cells/well and opsonized with antibodies in triplicate at the indicated final concentration for 30 min at room temperature. Effector cells at an effector to target (E/T) cell ratio of 5:1 were cocultured for 4 h and lactate dehydrogenase (LDH) activity was measured using the Cytotoxicity Detection kit (CytoTox-ONE, Promega). The percentage of maximal lysis was calculated as follows:

$$\mathrm{ADCC}(\%) = \frac{(\text{effector cells} + \text{target cells} + \text{antibody}) - (\text{effector cells} + \text{target cells})}{(\text{target cells} + \text{Triton X–100}) - \text{target cells}} \times 100\%$$

Primary tumor cells ADCC: ^{51}Cr release. Fresh unstimulated PBMC from patients and healthy donors were isolated as described (27). Donor PBMC typically contained 60% $CD3^+$ T cells, 10% to 20% $CD56^+$ NK cells, and 10% $CD14^+$ monocytes; PBMC samples from patients with ALL contained 95% tumor cells, and MCL bone aspirates contained 80% tumor cells. The viability of cells tested by trypan blue exclusion was higher than 95%. ADCC was measured with a ^{51}Cr release assay as described (27), except that 100 μCi of $^{51}Cr/10^6$ cells was used, E/T cell ratio was 80:1, and maximal ^{51}Cr release was determined with Triton X-100 (Sigma-Aldrich). The percentage of maximal lysis was calculated according to the equation above.

Phagocytosis. Macrophage ADCP was determined by flow cytometry as described (28), except that RS4;11 or SUP-B15 cells were used as targets and target cells were labeled with PKH67 (Sigma-Aldrich) or 5-(and-6)-carboxyfluorescein succinimidyl ester (Molecular Probes).

Proliferation and apoptosis. Proliferation and apoptosis assays were done using SU-DHL-6 cells in the presence of antibodies cross-linked by FcγRIIIa-GST. Reacti-Bind streptavidin-coated plates (Thermo Scientific) were coated with 0.5 μg/mL of biotinylated anti-GST antibody (U.S. Biologicals). FcγRIIIa-GST (1 μg/mL), antibodies at the indicated concentrations, and 6×10^3 SU-DHL-6 cells were added to a final volume of 100 μL in RPMI 1640/20% FBS. In the proliferation assay, samples were incubated for 72 h at 37°C, and viability (measured as

[3] M.J. Bernett, G.L. Moore, S. Karki, I. Vostiar, J.O. Richards, E. Pong, E.A. Zhukovsky, and J.R. Desjarlais, manuscript in preparation.

relative ATP luminescence) was detected using the CellTiter-Glo Luminescent Cell Viability assay kit (Promega) on a Topcount luminometer (Perkin-Elmer).

Caspase activation and Annexin V staining assays were used to detect apoptosis. For the caspase activation assay, samples were incubated for 48 h and analyzed with the Homogeneous Caspases assay kit (Roche Diagnostics). Data were acquired on a Victor2 Multi-Label reader (Perkin-Elmer). For the Annexin V assay, cells were labeled with Annexin V-PE using Apoptosis Detection kit Plus (BioVision) and 5 μg/mL of 7-amino-actinomycin D (Invitrogen). Data were analyzed on a FACSCanto II (BD Biosciences).

Relative ATP luminescence (%), caspase activity (%), and Annexin V^+ cells (%) were calculated as the ratio of signal elicited at a given antibody concentration to signal with no antibody present.

Lymphoma xenograft models. Prophylactic tumor studies were performed at, and according to procedures approved by, the Southern Research Institute's Institutional Animal Care and Use Committee (IACUC). Six- to 8-week-old female C.B-17 severe combined immunodeficient (SCID) mice (Charles River Laboratories) were implanted s.c. with either 10^7 Raji or 5×10^6 Ramos lymphoma cells. Mice were randomly placed into five groups (n = 10/group). On day 3 post-tumor cell implant and on days 6, 10, and 13, mice were injected i.p. with 1, 3, or 10 mg/kg of XmAb5574, 10 mg/kg of XmAb isotype control, or PBS. Palpable tumors were measured twice per week with calipers; tumor volumes were calculated as (length × $width^2$) / 2.

Established tumor studies were performed at Xencor according to procedures approved by Xencor's IACUC. Nine-week-old female C.B-17 SCID mice (Taconic) were injected s.c. with 2.5×10^6 Ramos cells. On day 14 post-cell implantation, mice bearing tumors between 30 and 130 mm^3 were placed into groups such that each group had the same mean tumor volume (82–84 mm^3; n = 10/group). Mice were injected i.p. with 10 mg/kg antibodies or PBS twice per week for 2 weeks; tumors were measured twice per week with calipers and volumes calculated as $\pi/6$ (length × width × height).

Data analysis. For *in vivo* studies, differences between groups were calculated using the nonparametric Mann-Whitney U test. $P < 0.05$ was considered significant.

Results

We previously reported that Fc-engineered variants of IgG1 optimized for FcγR affinity exhibit markedly enhanced ADCC in the context of several antibodies (anti-HER-2, anti-CD20, and anti-CD52; ref. 19). The Fc variant with S239D/I332E mutations was one of the most effective. Therefore, we applied these Fc mutations to generate a cytotoxic anti-CD19 antibody. The Fv domain from a mouse anti-CD19 antibody (clone 4G7; ref. 23) was humanized and affinity-matured, and combined with a human Fc domain containing the S239D/I332E mutations to increase FcγR binding and enhance ADCC. We refer to this Fc-engineered humanized anti-CD19 antibody as XmAb5574.

XmAb5574 displays increased FcγR binding affinity. To confirm that the S239D/I332E mutations enhance FcγR binding in the context of an anti-CD19 antibody, we determined the FcγR binding affinity of XmAb5574 and compared it to an IgG1 analogue (anti-CD19 IgG1), which contains the same Fv domain as XmAb5574, but has a native human IgG1 Fc. K_as were determined by measuring SPR on a Biacore biosensor (Fig. 1*A*). The S239D/I332E mutations elicited a profound increase in affinity to all human FcγRs, with the greatest enhancement of binding observed for the activating receptor FcγRIIIa, and particularly its low-affinity 158F allotype. K_as were also determined for an anti-CD19 Fc-KO (G236R/L328R), which was engineered to disrupt Fc receptor interactions for use as a control lacking effector function while retaining Fv-mediated signaling. The Fc-KO showed 630-fold reduced binding to FcγRI and had no detectable binding to FcγRIIa, FcγRIIb, and FcγRIIIa.

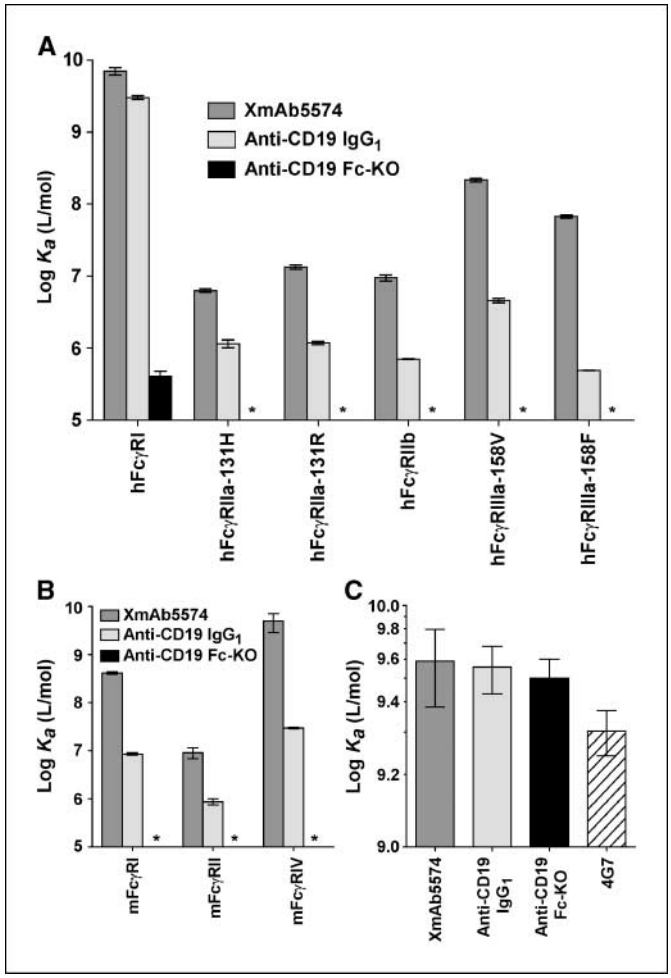

Figure 1. XmAb5574 exhibits dramatically increased binding affinity for human and mouse FcγRs, and retains high affinity to CD19 antigen. FcγR binding was determined by Biacore analysis. Equilibrium dissociation constants (K_ds) were obtained from Langmuir fits of the Biacore data, and affinities for each of the FcγRs were plotted as the log of the affinity constant, K_a. *A,* XmAb5574 showed significantly enhanced binding to all human FcγRs compared with the IgG1 analogue as follows: FcγRI, 2-fold; FcγRIIa-131H, 6-fold; FcγRIIa-131R, 11-fold; FcγRIIb, 13-fold; FcγRIIIa-158V, 47-fold; and FcγRIIIa-158F, 136-fold. Anti-CD19 Fc-KO binding was either completely eliminated (*, FcγRIIa, FcγRIIb, and FcγRIIIa) or drastically reduced (FcγRI). *B,* XmAb5574 enhanced binding to mouse FcγRs as follows: FcγRI, 50-fold; FcγRII, 11-fold; and FcγRIV, 148-fold. The Fc-KO showed no detectable binding to any mouse FcγRs. Because mouse FcγRIII sensorgrams did not conform to the standard binding model, the fold increase of XmAb5574 FcγRIII binding relative to the IgG1 analogue was calculated as the ratio of maximal signal at 20 s post-antibody injection. A 3.5-fold increase was obtained (data not shown). *C,* binding to CD19 antigen was measured using a Raji cell–based competitive binding assay with Alexa Fluor 647–labeled XmAb5574. *Columns,* averages of three or more independent experiments; *bars,* SD (*A–C*).

To evaluate the antitumor efficacy of XmAb5574 in mouse xenograft models, it was important to assess whether XmAb5574 also increased binding to mouse FcγRs. Similar to our observations with human FcγRs, XmAb5574 exhibited increased affinity for all mouse Fc receptors relative to the IgG1 analogue, and the anti-CD19 Fc-KO showed no detectable binding to any mouse FcγRs (Fig. 1*B*).

We also characterized the CD19 binding properties of XmAb5574 by determining K_as in a Raji cell–based competitive binding assay.

As shown in Fig. 1*C*, XmAb5574, anti-CD19 IgG1, and the anti-CD19 Fc-KO all bind CD19 antigen with similar K_as, and these are approximately 2-fold higher than the K_a for the parent mouse anti-CD19 antibody (4G7). Thus, XmAb5574 has substantially increased binding affinity for both human and mouse FcγRs and has high affinity to the CD19 antigen.

XmAb5574 induces minimal receptor internalization. Because the reported rate of internalization of CD19 on anti-CD19 binding varies widely, and because internalization of the target antigen may affect antibody effector function (29), we compared the internalization of XmAb5574 to an anti-CD22 antibody and to rituximab (anti-CD20), which have been shown to induce either fast or slow rates of internalization, respectively (30). Antibodies were directly labeled with europium and then incubated with Raji cells, which express high levels of all three antigens (31). Dissociation of antibody from cell surface CD19 is a function of antigen affinity, and as expected, increased with time, resulting in an increased amount of europium-labeled antibody in the supernatant and a concomitant decrease in the total cell-associated fraction (Fig. 2*A*). Binding of XmAb5574 resulted in very little internalization over 4 h; maximum internalization occurred at about 2 h and was only 6% (Fig. 2*B*). Anti-CD20 displayed a similar profile and maximum, with <3% internalized (Figs. S1*A* and 2*B*). In contrast, anti-CD22 facilitated rapid internalization, exhibiting a maximum of 37% internalized at 30 min (Figs. S1*B* and 2*B*). These data indicate that XmAb5574 binding to CD19 induces minimal internalization which should not significantly affect effector functions.

XmAb5574 enhances ADCC and ADCP. To determine whether the increased FcγR affinity of XmAb5574 translates into enhancements in immune effector functions, we first performed *in vitro* ADCC assays using purified IL-2–activated NK cells and cell lines spanning a broad range of human lymphomas and leukemias [Burkitt's lymphoma, CLL, HCL, $CD19^+$ chronic myeloid leukemia (CML), diffuse large B-cell lymphoma (DLBCL), and ALL] and expressing different levels of CD19 antigen (15,000–105,000 molecules/cell). XmAb5574 markedly enhanced ADCC in all tumor cell lines assayed (Fig. 3*A*), significantly increasing both efficacy (maximal lysis) and potency (EC_{50}) relative to the IgG1 analogue. EC_{50}s for XmAb5574 ranged from 0.1 to 1.0 ng/mL, representing increases in potency of 100-fold to 1,000-fold over the IgG1 analogue. Maximal lysis for XmAb5574 ranged from 25% to 90%, and no correlation with cell surface CD19 expression was observed; the IgG1 analogue was much less efficacious (consistent with previous observations; ref. 32), exhibiting either no or 2-fold to 3-fold less ADCC (except RS4;11 cells). Notably, XmAb5574 induced substantial lysis even in cell lines in which the IgG1 analogue was virtually inactive (SU-DHL-6 and Raji). ADCC for the anti-CD19 Fc-KO was also assayed and no lysis was observed (Fig. S2), indicating that FcγR engagement is required for antibody effector function. The XmAb isotype control antibody also induced no detectable cell lysis, indicating that increased binding to FcγR alone in the absence of specific Fv-antigen interaction was insufficient to induce ADCC.

To determine whether XmAb5574 mediated increased ADCC not only against cell lines but also against primary tumors, we performed an assay with tumor cells from patients with ALL or MCL using fresh unfractionated and unstimulated PBMCs. The ADCC averages of three PBMC donors are presented (Fig. 3*B* and *C*). XmAb5574 enhanced ADCC in both ALL and MCL cells, in striking contrast to the IgG1 analogue, which showed no detectable ADCC. The lack of measurable ADCC for the IgG1 analogue underscores the resilience of primary tumor cells as was also observed in two of the nine tumor cell lines (Fig. 3*A*).

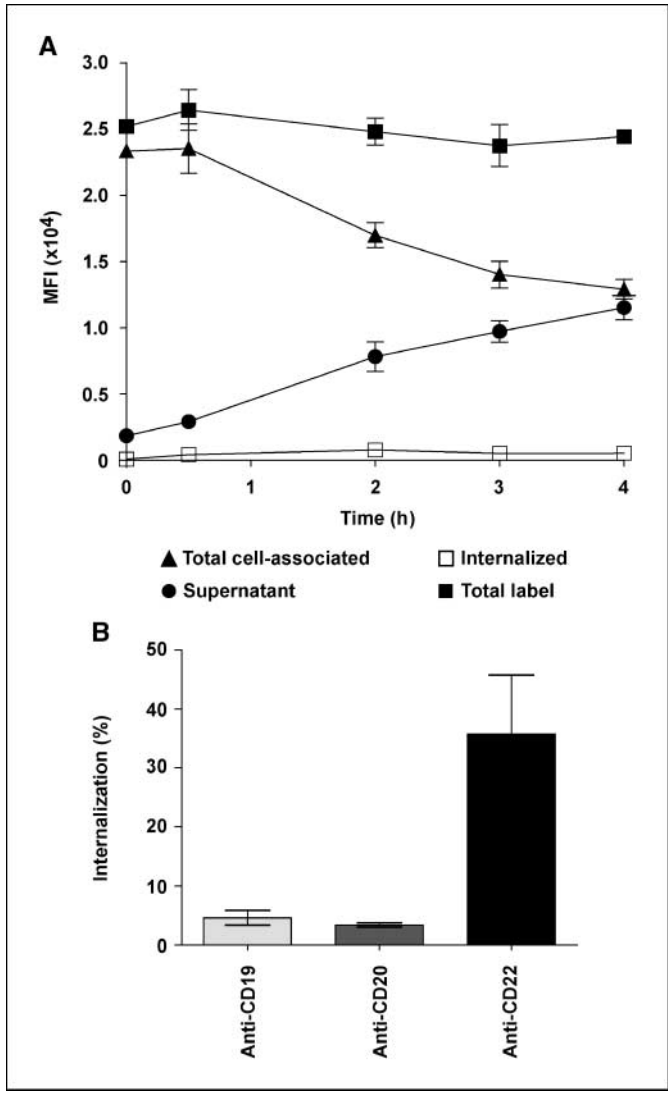

Figure 2. XmAb5574 facilitates minimal CD19 internalization. Internalization of XmAb5574 was compared with that of anti-CD22 (RFB4) and anti-CD20 (rituximab). Europium-labeled antibodies were incubated with Raji cells and europium fluorescence was determined at multiple time points. *A,* time course showing localization of europium-labeled XmAb5574 in the total cell-associated fraction (surface bound plus internalized antibody) and in the supernatant (antibody dissociated from cell surface). Internalized antigen-antibody complexes were estimated by lowering the pH of the total cell-associated fraction to remove surface-bound antibodies and measuring cell-associated fluorescence again. Total label was calculated by summing the total cell-associated, supernatant, and internalized fractions; values totaled to within 10% of europium label used. *B,* percentage of internalization at maximum for each antibody. Data were obtained in triplicate; *bars,* SD (*A* and *B*).

To assess the effect of XmAb5574 on phagocytosis, we performed ADCP assays with monocyte-derived macrophages and two ALL cell lines. XmAb5574 increased phagocytosis efficacy by approximately 10-fold relative to the IgG1 analogue (Fig. 4), substantially lower than the enhancement of ADCC (1,000-fold). As discussed later, this difference may be a reflection of different FcγRs responsible for NK cell versus macrophage-associated effector functions. Finally, XmAb5574 did not exhibit any CDC activity on Ramos or Raji cells (data not shown).

Thus, XmAb5574 substantially enhanced immune effector function, augmenting ADCC up to 1,000-fold relative to the IgG1 analogue in a broad range of B-lymphoma and leukemia cell lines and in primary tumor cells, and eliciting a 10-fold enhancement in macrophage-mediated ADCP.

XmAb5574 enhances antiproliferative apoptotic activity. Because previous reports showed that anti-CD19 antibodies are antiproliferative (33, 34), we measured the effect of XmAb5574 on tumor cell viability. We also assessed the effect of Fc binding on antiproliferative activity by comparing the effects of XmAb5574 with those of the anti-CD19 IgG1 analogue and the anti-CD19 Fc-KO. Secondary cross-linking antibodies are often used *in vitro* to mimic the *in vivo* environment in which antibody cross-linking occurs via binding to FcγRs on immune effector cells (35). As a more direct mimic of these effects, we used an FcγRIIIa-158V-GST fusion receptor as a cross-linker (the GST domain spontaneously dimerizes) instead of the nonspecific antihuman Fc antibodies used in such assays. The cross-linked antibodies were incubated with SU-DHL-6 cells and cell titers were analyzed using a cell viability assay. XmAb5574 exhibited more potent antiproliferative activity than the IgG1 analogue (Fig. 5*A*), indicating the importance of optimized Fc binding to FcγRs in mediating this effect. However, the activity of the Fc-KO was similar to the IgG1 analogue, suggesting that the antiproliferative activity is not absolutely dependent on cross-linking, but can be amplified by it. XmAb5574 also displayed antiproliferative activity in Raji and Ramos cell lines (data not shown).

We also performed Annexin V staining and caspase activation assays to elucidate the mechanism of antiproliferative effects induced by XmAb5574, and found them to be due to caspase-mediated apoptosis (Fig. 5*B* and *C*). As in the proliferation assay, XmAb5574 was more potent than the IgG1 analogue, which was comparable to the anti-CD19 Fc-KO. The enhanced FcγR binding of XmAb5574 may have augmented antibody cross-linking and thus facilitated cell surface CD19 cross-linking, leading to increased apoptosis. Therefore, XmAb5574 showed potent antiproliferative effects due to caspase-induced apoptosis, and these effects were more pronounced than those seen with the IgG1 analogue.

XmAb5574 inhibits lymphoma growth in SCID mouse xenograft models. We examined the *in vivo* antitumor effect of XmAb5574, administered either prophylactically or in an established tumor model. In prophylactic studies, mice were implanted s.c. with Ramos or Raji Burkitt's lymphoma cells, then injected i.p. with XmAb5574 (1, 3, or 10 mg/kg), XmAb isotype control, or vehicle on days 3, 6, 10, and 13. In both prophylactic studies, all three XmAb5574-treated groups showed a statistically significant inhibition of tumor growth compared with XmAb isotype–treated or vehicle-treated controls (Fig. 6*A* and *B*). On day 42 of the Ramos study, XmAb5574 at 1, 3, or 10 mg/kg reduced tumor growth by 44%, 59%, and 69% relative to controls,

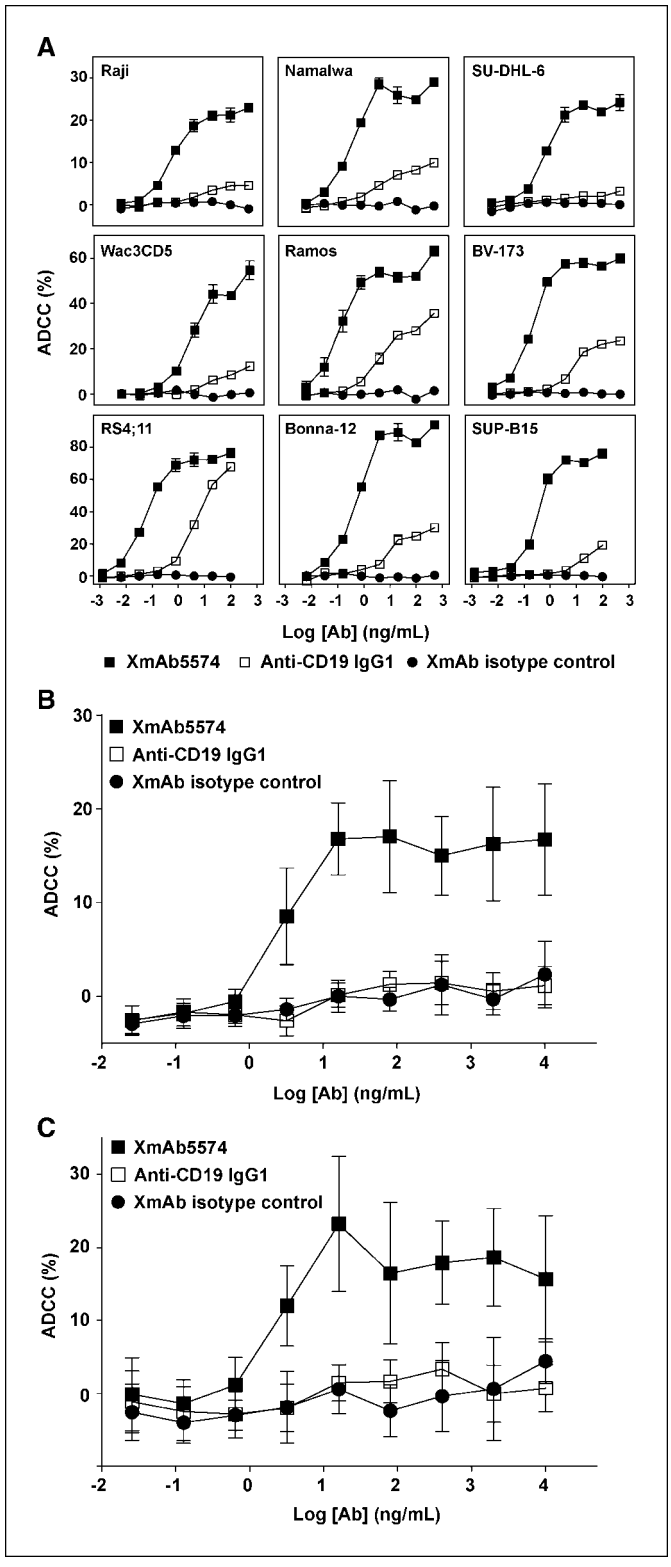

Figure 3. XmAb5574 enhances ADCC potency and efficacy in multiple tumor cell lines (*A*) and in patient-derived primary tumor tissue (*B* and *C*). *A,* ADCC was measured with an LDH release assay using purified IL-2–activated NK cells as effectors and nine lymphoma or leukemia cell lines as targets. Cell surface CD19 was determined using QIFIKIT (DakoCytomation, Inc.) and murine 4G7 antibody (BD Biosciences) according to the manufacturer's protocol. The target cell lines used and the corresponding number of CD19 molecules/cell (in parentheses) were as follows: Burkitt's lymphoma, Raji (105,000), Namalwa (37,000), Ramos (56,000); DLBCL, SU-DHL-6 (15,000); CLL, WaC3CD5 (38,000); CML, BV-173 (80,000); ALL, RS4;11 (43,000), SUP-B15 (49,000); and HCL, Bonna-12 (29,000). Target cells were opsonized with antibodies and mixed with NK cells at a cell ratio of 1:5; LDH release was measured 4 h later. Data were obtained in triplicate; *bars,* SD. *B* and *C,* target primary tumor cells were obtained from patients with ALL (*B*) or MCL (*C*). All samples showed high CD19 expression. Tumor cells were labeled with ^{51}Cr (100 $\mu Ci/10^6$ cells), opsonized with antibodies, and mixed with PBMCs at a cell ratio of 1:80 for 4 h; ADCC was determined using a ^{51}Cr release. *Points,* averages of three experiments from three different PBMC donors; *bars,* SD.

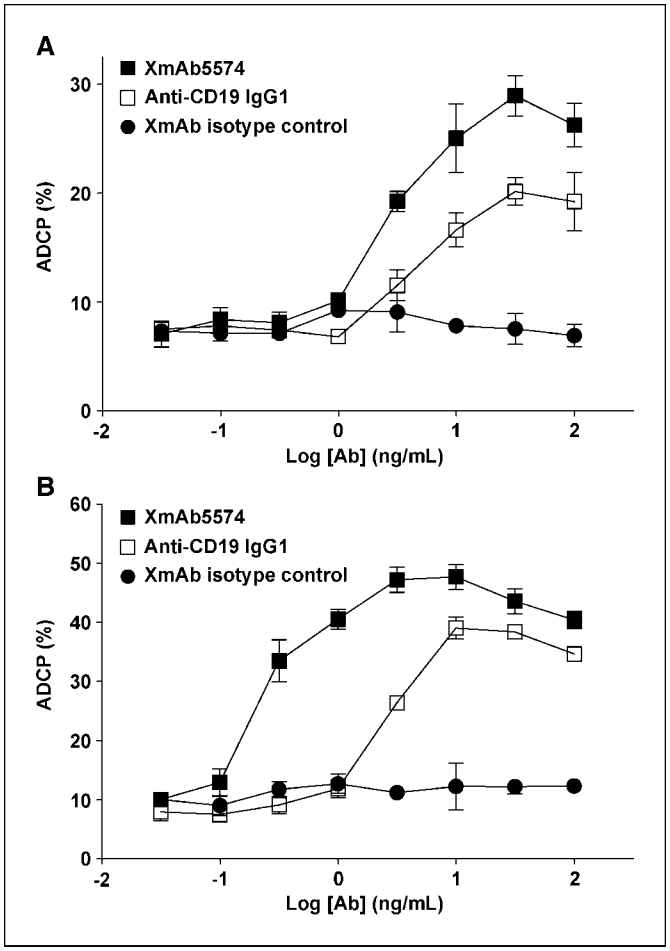

Figure 4. XmAb5574 enhances macrophage phagocytosis in B-leukemia cell lines. ADCP was determined by flow cytometry using RS4;11 (*A*) or SUP-B15 (*B*) cells as targets and monocyte-derived macrophages (MDM) as effector cells. Macrophages were differentiated from purified CD14+ cells by culturing in macrophage colony-stimulating factor for 5 d. Target cells were fluorescently labeled with PKH67 or 5-(and-6)-carboxyfluorescein succinimidyl ester, opsonized with antibodies, and cocultured with monocyte-derived macrophages at an E/T ratio of 4:1 for 4 h. Cells were then double-stained with anti–CD11b-APC and anti–CD14-APC and analyzed by flow cytometry; percentage of ADCP was calculated as the number of double-positive cells divided by the total number of tumor cells. Data were obtained in triplicate; *bars,* SD.

respectively. In the Raji study, XmAb5574 reduced tumor growth by >80% at all three doses compared with vehicle or XmAb isotype controls, and tumors were completely eradicated in 10% to 30% of the mice. In both studies, we found no difference between the XmAb isotype–treated and vehicle-treated controls, suggesting that the S239D/I332E mutations did not induce nonspecific activation of immune effector cells.

Next, we assessed the efficacy of XmAb5574 in an established tumor model. To determine the contribution of FcγR binding in mediating antitumor effects, we compared the *in vivo* activities of XmAb5574, the anti-CD19 Fc-KO, and the IgG1 analogue. SCID mice were implanted with Ramos lymphoma cells, and tumors were allowed to grow to a mean volume of ~80 mm^3 before twice weekly treatment with 10 mg/kg was started on day 14. By day 27, all three anti-CD19 antibodies caused a significant reduction in tumor growth compared with vehicle (Fig. 6*C* and Fig. S3); XmAb5574 elicited the most dramatic effect, reducing tumor growth by 80% on day 27 ($P < 0.0001$). The fact that the anti-CD19 Fc-KO also significantly decreased tumor growth (26%) indicates that mechanisms other than those mediated through FcγRs contribute to antitumor efficacy. However, as evidenced by the markedly increased inhibition observed for XmAb5574 relative to

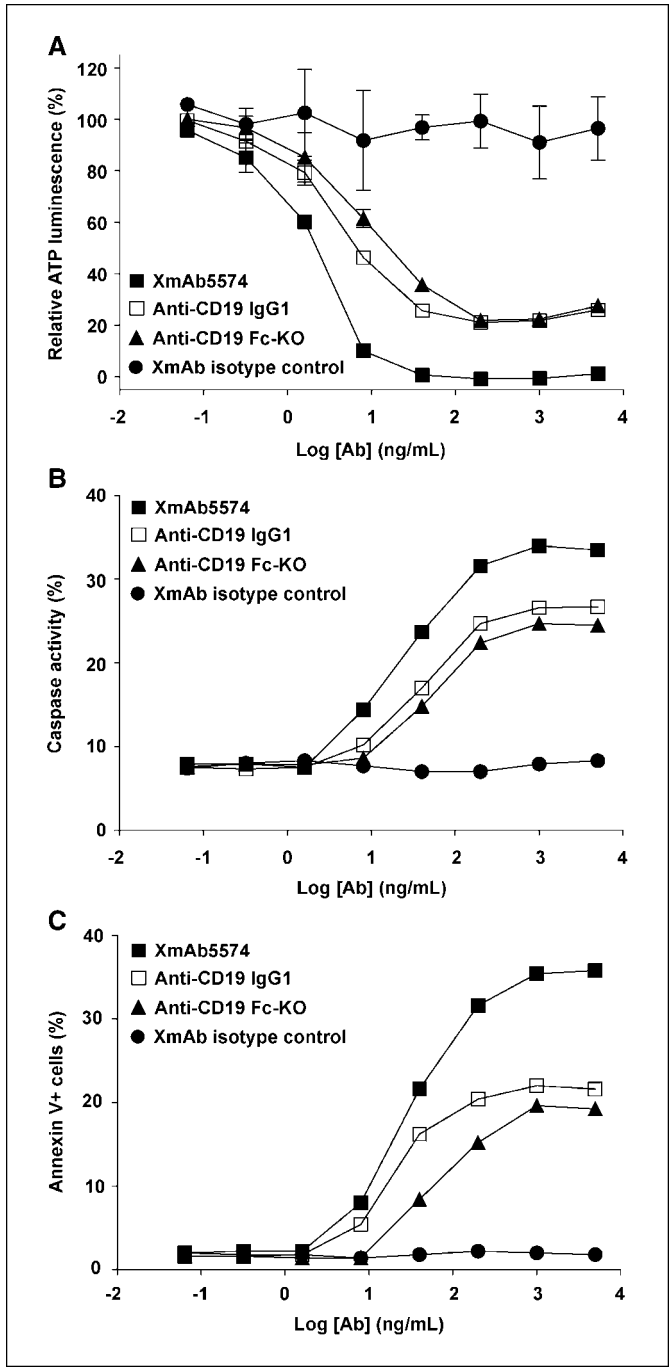

Figure 5. XmAb5574 exhibits robust antiproliferative activity due to caspase-mediated apoptosis. Studies were performed on SU-DHL-6 cells using a human FcγRIIIa-GST fusion receptor to provide antibody cross-linking. *A,* proliferation assay: cross-linked antibodies were incubated with 6×10^3 cells for 72 h, and cell titers were analyzed using a luminescent cell viability assay. Data were obtained in triplicate; *bars,* SD. *B* and *C,* apoptosis was assayed using caspase activation (*B*) and Annexin V staining (*C*). Cross-linked antibodies were incubated with SU-DHL-6 cells for 48 h. Caspase activity was quantitated using a fluorometric assay. For the Annexin V assay, cells were labeled with Annexin V-PE and 7-amino-actinomycin D, and fluorescence was analyzed by flow cytometry. Data are from a single experiment (*B* and *C*).

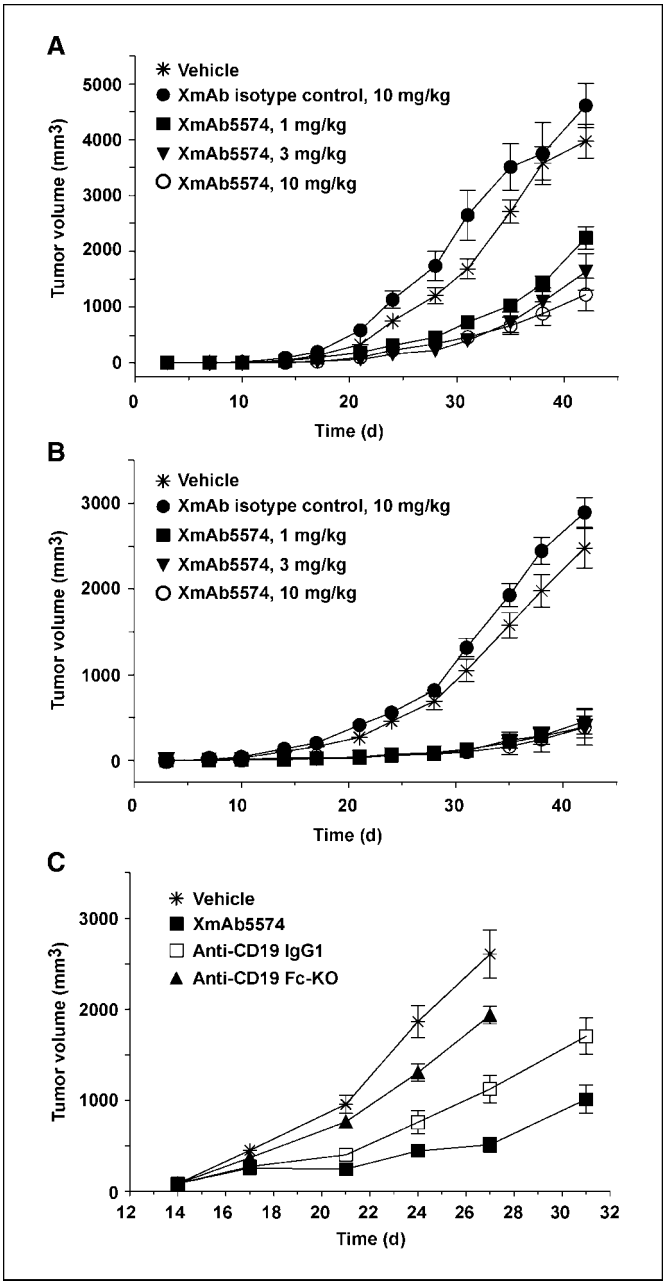

Figure 6. XmAb5574 inhibits lymphoma growth in prophylactic and established SCID mouse xenograft models. *A* and *B,* prophylactic studies. SCID mice were implanted s.c. with Ramos (*A*) or Raji (*B*) cells, then injected i.p. with XmAb5574 (1, 3, or 10 mg/kg), 10 mg/kg XmAb isotype control, or vehicle on days 3, 6, 10, and 13. *C,* Ramos established tumor study. SCID mice were implanted with lymphoma cells and tumors were allowed to grow to a mean volume of 80 mm^3 before biweekly i.p. treatment with 10 mg/kg for 2 wk, starting on day 14. At day 27, XmAb5574, anti-CD19 IgG1, and the anti-CD19 Fc-KO significantly reduced tumor growth compared with vehicle: 80% ($P < 0.0001$), 57% ($P = 0.0014$), and 26% ($P = 0.0062$), respectively. XmAb5574 significantly reduced tumor growth relative to the anti-CD19 Fc-KO ($P < 0.0001$) and to anti-CD19 IgG1 ($P = 0.0029$), and a significant difference was seen between anti-CD19 IgG1 and the anti-CD19 Fc-KO ($P = 0.0011$). Vehicle and anti-CD19 Fc-KO mice were sacrificed on day 27 according to IACUC protocol. *Bars,* SE; $n = 10$ mice/group (*A–C*).

the anti-CD19 Fc-KO (80% versus 26%) and to a lesser degree for the IgG1 analogue versus the Fc-KO (57% versus 26%), most of the inhibition seems to be Fc-mediated. Finally, a significant difference was also seen between XmAb5574 and the IgG1 analogue (80% versus 57%; $P = 0.0029$), demonstrating the effect of increased affinity for FcγR due to the S239D/I332E Fc mutations.

These results show that XmAb5574, in addition to having strong antitumor effects *in vitro*, also has potent antitumor activity *in vivo* on human lymphoma xenografts. XmAb5574 inhibits tumor growth in mice via both FcγR-dependent and FcγR-independent mechanisms, and this inhibition is significantly enhanced relative to the IgG1 analogue.

Discussion

B-cell depletion has been a successful strategy in the treatment of B-cell malignancies (36). The success of the anti-CD20 antibody rituximab in combination with chemotherapy has made this regimen the new standard of care for the treatment of B-cell cancers. The broad use of rituximab has shown that primary monotherapy with this agent, or retreatment of relapsed cases, is efficacious in approximately half of the patients (7). These failures of rituximab have been attributed to a variety of mechanisms (37), including a loss of CD20 expression on tumor cells, observed both in relapsed patients (5, 6) and in mouse xenograft models (38). CD19 is an attractive alternative target for the immunotherapy of lymphoproliferative disorders, due to its expression on a wide range of lymphomas and leukemias, including some early B-cell malignancies that do not express CD20 (2, 9). The potential for anti-CD19 antibodies to be effective against a broader range of B-cell tumors, their potential for overcoming rituximab-specific resistance, and the positive early clinical results with CD19 bispecific antibodies (16) make anti-CD19 antibodies especially promising candidates for therapeutic development.

Although early studies showed that unmodified anti-CD19 antibodies induced B-cell depletion, their clinical efficacy was limited (8, 15), and consequently, clinical trials focused on anti-CD19 immunotoxin conjugates (10, 39). To maximize the cytotoxic potential of an unmodified antibody, multiple modes of tumor cell killing must be engaged: immune effector function (ADCC, ADCP, or CDC) and growth inhibition mechanisms (apoptosis or cell cycle arrest). Data from both murine and human studies have shown that FcγR engagement, a major component of the effector function of antibodies, is the critical factor for optimal antitumor activity. Antibodies such as rituximab and trastuzumab have been reported to lose most of their antitumor activity in mice lacking the common γ chain required by all mouse activating FcγRs (40). Patient FcγR polymorphism analyses have shown that the affinity preference of IgG1 antibodies for the FcγRIIIa-158V versus 158F allotype correlates with improved progression-free survival in lymphoma and breast cancer patients treated with antibodies against CD20 (41, 42) or HER-2/*neu* (43), respectively. Furthermore, a series of studies in mouse models and human clinical trials have corroborated these fundamental observations (44, 45) and collectively indicate that higher FcγR affinity is associated with more efficient tumor clearance.

Previously, we showed that modification of the Fc domain to increase FcγR binding results in a dramatic enhancement in ADCC (19), and others have shown that anti-CD19 antibodies deplete B cells in an FcγR-dependent fashion (9). Here, we report that XmAb5574, an anti-CD19 antibody engineered for high affinity to human FcγRs, not only increases ADCC, but also increases ADCP and apoptosis, and enhances tumor inhibition in mouse xenograft models. XmAb5574 has high affinity to human CD19 and substantially increased affinity for human FcγRIIIa and FcγRIIa

(100-fold and 10-fold, respectively). The higher affinity for FcγRIIIa translates directly into substantially enhanced ADCC against a broad range of leukemia and lymphoma cell lines and primary tumor cells. The increased FcγR affinity of XmAb5574 seems to be critical for maximal effectiveness because the IgG1 analogue displayed no or minimal levels of ADCC. The substantial increase in macrophage phagocytosis attributed to the S239D/I332E Fc substitutions is also of significance, given the growing evidence that macrophage-associated effector functions may be essential for *in vivo* antibody activity (46, 47). The observed difference in the XmAb5574-mediated enhancement of ADCC versus ADCP (1,000-fold versus 10-fold) may be a reflection of different FcγRs responsible for either NK cell or macrophage-associated effector functions. The Fc substitutions increase binding to FcγRIIIa 10-fold more than to FcγRIIa. In contrast to NK cells, which express only FcγRIIIa, macrophages express both of the low-affinity activating receptors, FcγRIIIa and FcγRIIa. Therefore, the more modest increase of ADCP conferred by these mutations may reflect the dominance of FcγRIIa in mediating phagocytosis, consistent with previous observations (28).

Fc engineering of XmAb5574 also resulted in enhanced apoptosis relative to the IgG1 analogue and the anti-CD19 Fc-KO. Although antibody-elicited apoptosis depends on the direct interaction of antibodies with their cell surface targets, these effects may be amplified by antibody cross-linking via FcγR on effector cells (35). Thus, optimization of Fc-binding to FcγRs in XmAb5574 may also result in more efficient cross-linking to mediate the enhanced apoptosis. This mechanism is supported by the observation that no difference in apoptotic activity is detected between XmAb5574 and the IgG1 analogue when cross-linked via a non–FcγR-binding epitope (data not shown). Thus, increased Fc binding to FcγRs substantially enhanced both effector-mediated killing and apoptotic activity of the resultant antibody, affording XmAb5574 with multiple mechanisms of tumor cytotoxicity.

XmAb5574 treatment of established human lymphoma resulted in significant inhibition of tumor growth relative to vehicle and the anti-CD19 Fc-KO, and notably was more inhibitory than the anti-CD19 IgG1 analogue. Although the anti-CD19 Fc-KO exhibited detectable tumor inhibition, the activity was severely attenuated relative to either XmAb5574 or the IgG1 analogue, adding to observations made by others (40, 46–48) and further emphasizing the importance of FcγR engagement for maximal antitumor activity. The S239D/I332E substitutions in XmAb5574 increased affinity for all the murine FcγRs, with a particularly strong enhancement for mouse activating FcγRI and FcγRIV, the latter of which has been strongly implicated in the *in vivo* activity of antibodies (46). Consistent with its enhanced affinity for murine FcγRs relative to anti-CD19 IgG1, XmAb5574 also showed more tumor inhibition than its IgG1 analogue, emphasizing the importance of Fc engineering for enhanced *in vivo* efficacy. These observations are similar to those made for an anti-CD32b antibody with enhanced affinity for mouse FcγRIV (21). However, it is worth noting that extrapolation of the mouse results to human clinical efficacy is not straightforward because of disparities between mouse and human immune systems, including differences in FcγRs and cell types responsible for immune function (17). Nevertheless, taken together, these promising results support further development of XmAb5574 for the therapy of human lymphoma and leukemia.

Internalization of CD19 upon antibody binding is a matter of controversy. Several reports conclude that anti-CD19 antibody binding either facilitates (30, 49) or has no effect on internalization (50, 51). These contradictory results may be reconciled by differences in CD21 expression levels, which are reportedly inversely correlated with internalization (31). Because antibody effector function could be affected by internalization of the antibody-antigen complex, we studied internalization facilitated by XmAb5574 and showed that very little occurs. Moreover, it is obvious from the *in vivo* results that the degree of internalization observed was not sufficient to prevent the dramatic tumor inhibition seen in the mouse lymphoma models.

The humanized and affinity-optimized anti-CD19 antibody XmAb5574 was Fc-engineered to enhance immune cell–mediated effector functions. It also possesses increased apoptotic activity that may be facilitated via its augmented FcγR interactions. Thus, XmAb5574 exhibits multiple modes of potent tumor cytotoxicity that are substantially increased relative to native IgG1 anti-CD19 antibodies. This activity profile should maximize the chances for successful clinical application of XmAb5574 in a diverse patient population.

Disclosure of Potential Conflicts of Interest

The authors are employees of and have ownership interest in Xencor, with the exception of M. Peipp and R. Repp.

Acknowledgments

Received 6/16/2008; revised 7/24/2008; accepted 7/25/2008.

The costs of publication of this article were defrayed in part by the payment of page charges. This article must therefore be hereby marked *advertisement* in accordance with 18 U.S.C. Section 1734 solely to indicate this fact.

We thank Araz Eivazi, Bally Randhawa, and Chi-Ming Yu for technical contributions, Marie Ary for assistance with writing the article, and David Szymkowski for helpful discussions.

References

1. Tedder TF, Inaoki M, Sato S. The CD19-21 complex regulates signal transduction thresholds governing humoral immunity and autoimmunity. Immunity 1997; 6:107–18.
2. Anderson KC, Bates MP, Slaughenhoupt BL, Pinkus GS, Schlossman SF, Nadler LM. Expression of human B cell-associated antigens on leukemias and lymphomas: a model of human B cell differentiation. Blood 1984;63: 1424–33.
3. Ginaldi L, De Martinis M, Matutes E, Farahat N, Morilla R, Catovsky D. Levels of expression of CD19 and CD20 in chronic B cell leukaemias. J Clin Pathol 1998;51: 364–9.
4. Harris NL, Stein H, Coupland SE, et al. New approaches to lymphoma diagnosis. Hematology Am Soc Hematol Educ Program 2001:194–220.
5. Davis TA, Czerwinski DK, Levy R. Therapy of B-cell lymphoma with anti-CD20 antibodies can result in the loss of CD20 antigen expression. Clin Cancer Res 1999;5: 611–5.
6. Kennedy GA, Tey SK, Cobcroft R, et al. Incidence and nature of CD20-negative relapses following rituximab therapy in aggressive B-cell non-Hodgkin's lymphoma: a retrospective review. Br J Haematol 2002;119: 412–6.
7. Bello C, Sotomayor EM. Monoclonal antibodies for B-cell lymphomas: Rituximab and beyond. Hematology Am Soc Hematol Educ Program 2007;2007:233–42.
8. Vlasveld LT, Hekman A, Vyth-Dreese FA, et al. Treatment of low-grade non-Hodgkin's lymphoma with continuous infusion of low-dose recombinant interleukin-2 in combination with the B-cell-specific monoclonal antibody CLB-CD19. Cancer Immunol Immunother 1995;40:37–47.
9. Yazawa N, Hamaguchi Y, Poe JC, Tedder TF. Immunotherapy using unconjugated CD19 monoclonal antibodies in animal models for B lymphocyte malignancies and autoimmune disease. Proc Natl Acad Sci U S A 2005; 102:15178–83.
10. Grossbard ML, Lambert JM, Goldmacher VS, et al. Anti-B4-blocked ricin: a phase I trial of 7-day continuous infusion in patients with B-cell neoplasms. J Clin Oncol 1993;11:726–37.

11. Rowland AJ, Pietersz GA, McKenzie IF. Preclinical investigation of the antitumour effects of anti-CD19-idarubicin immunoconjugates. Cancer Immunol Immunother 1993;37:195–202.

12. Sapra P, Allen TM. Internalizing antibodies are necessary for improved therapeutic efficacy of antibody-targeted liposomal drugs. Cancer Res 2002;62:7190–4.

13. Molhoj M, Crommer S, Brischwein K, et al. CD19-/CD3-bispecific antibody of the BiTE class is far superior to tandem diabody with respect to redirected tumor cell lysis. Mol Immunol 2007;44:1935–43.

14. Bruenke J, Barbin K, Kunert S, et al. Effective lysis of lymphoma cells with a stabilised bispecific single-chain Fv antibody against CD19 and FcgRIII (CD16). Br J Haematol 2005;130:218–28.

15. Hekman A, Honselaar A, Vuist WM, et al. Initial experience with treatment of human B cell lymphoma with anti-CD19 monoclonal antibody. Cancer Immunol Immunother 1991;32:364–72.

16. Bargou R, Leo E, Zugmaier G, et al. Tumor regression in cancer patients by very low doses of a T cell–engaging antibody. Science 2008;321:974–7.

17. Desjarlais JR, Lazar GA, Zhukovsky EA, Chu SY. Optimizing engagement of the immune system by anti-tumor antibodies: an engineer's perspective. Drug Discov Today 2007;12:898–910.

18. Bowles JA, Wang SY, Link BK, et al. Anti-CD20 monoclonal antibody with enhanced affinity for CD16 activates NK cells at lower concentrations and more effectively than rituximab. Blood 2006;108:2648–54.

19. Lazar GA, Dang W, Karki S, et al. Engineered antibody Fc variants with enhanced effector function. Proc Natl Acad Sci U S A 2006;103:4005–10.

20. Shields RL, Namenuk AK, Hong K, et al. High resolution mapping of the binding site on human IgG1 for FcgRI, FcgRII, FcgRIII, and FcRn and design of IgG1 variants with improved binding to the FcgR. J Biol Chem 2001;276:6591–604.

21. Stavenhagen JB, Gorlatov S, Tuaillon N, et al. Fc optimization of therapeutic antibodies enhances their ability to kill tumor cells *in vitro* and controls tumor expansion *in vivo* via low-affinity activating Fcg receptors. Cancer Res 2007;67:8882–90.

22. Tedder TF, Baras A, Xiu Y. Fcg receptor-dependent effector mechanisms regulate CD19 and CD20 antibody immunotherapies for B lymphocyte malignancies and autoimmunity. Springer Semin Immunopathol 2006;28:351–64.

23. Meeker TC, Miller RA, Link MP, Bindl J, Warnke R, Levy R. A unique human B lymphocyte antigen defined by a monoclonal antibody. Hybridoma 1984;3:305–20.

24. Lazar GA, Desjarlais JR, Jacinto J, Karki S, Hammond PW. A molecular immunology approach to antibody humanization and functional optimization. Mol Immunol 2007;44:1986–98.

25. Wu H, Pfarr DS, Johnson S, et al. Development of motavizumab, an ultra-potent antibody for the prevention of respiratory syncytial virus infection in the upper and lower respiratory tract. J Mol Biol 2007;368:652–65.

26. Cheng Y, Prusoff WH. Relationship between the inhibition constant (K1) and the concentration of inhibitor which causes 50 per cent inhibition (I50) of an enzymatic reaction. Biochem Pharmacol 1973;22:3099–108.

27. Peipp M, Schneider-Merck T, Dechant M, et al. Tumor cell killing mechanisms of epidermal growth factor receptor (EGFR) antibodies are not affected by lung cancer-associated EGFR kinase mutations. J Immunol 2008;180:4338–45.

28. Richards JO, Karki S, Lazar GA, Chen H, Dang W, Desjarlais JR. Optimization of antibody binding to FcgRIIa enhances macrophage phagocytosis of tumor cells. Mol Cancer Ther 2008;7:2517–27.

29. Chatenoud L, Bach JF. Antigenic modulation—a major mechanism of antibody action. Immunol Today 1984;5:20–5.

30. Press OW, Farr AG, Borroz KI, Anderson SK, Martin PJ. Endocytosis and degradation of monoclonal antibodies targeting human B-cell malignancies. Cancer Res 1989;49:4906–12.

31. Ingle GS, Chan P, Elliott JM, et al. High CD21 expression inhibits internalization of anti-CD19 antibodies and cytotoxicity of an anti-CD19-drug conjugate. Br J Haematol 2008;140:46–58.

32. Barbin K, Stieglmaier J, Saul D, et al. Influence of variable N-glycosylation on the cytolytic potential of chimeric CD19 antibodies. J Immunother (1997) 2006;29:122–33.

33. Benoit NE, Wade WF. Increased inhibition of proliferation of human B cell lymphomas following ligation of CD40, and either CD19, CD20, CD95 or surface immunoglobulin. Immunopharmacology 1996;35:129–39.

34. Bradbury LE, Kansas GS, Levy S, Evans RL, Tedder TF. The CD19/CD21 signal transducing complex of human B lymphocytes includes the target of antiproliferative antibody-1 and Leu-13 molecules. J Immunol 1992;149:2841–50.

35. Xu Y, Szalai AJ, Zhou T, et al. FcgRs modulate cytotoxicity of anti-Fas antibodies: implications for agonistic antibody-based therapeutics. J Immunol 2003;171:562–8.

36. Cheson BD. Monoclonal antibody therapy for B-cell malignancies. Semin Oncol 2006;33:S2–14.

37. Bonavida B. Rituximab-induced inhibition of anti-apoptotic cell survival pathways: implications in chemo/immunoresistance, rituximab unresponsiveness, prognostic and novel therapeutic interventions. Oncogene 2007;26:3629–36.

38. Nijmeijer B, van Schie MLJ, Willemze R, Falkenburg JHF. Rituximab and alemtuzumab in combination, but not alone, induce complete remissions in a preclinical animal model of primary human ALL: rationale for combination treatment [abstract]. Blood 2007;110:2833.

39. Tsimberidou AM, Giles FJ, Kantarjian HM, Keating MJ, O'Brien SM. Anti-B4 blocked ricin post chemotherapy in patients with chronic lymphocytic leukemia-long-term follow-up of a monoclonal antibody-based approach to residual disease. Leuk Lymphoma 2003;44:1719–25.

40. Clynes RA, Towers TL, Presta LG, Ravetch JV. Inhibitory Fc receptors modulate *in vivo* cytoxicity against tumor targets. Nat Med 2000;6:443–6.

41. Cartron G, Dacheux L, Salles G, et al. Therapeutic activity of humanized anti-CD20 monoclonal antibody and polymorphism in IgG Fc receptor FcgRIIIa gene. Blood 2002;99:754–8.

42. Weng WK, Levy R. Two immunoglobulin G fragment C receptor polymorphisms independently predict response to rituximab in patients with follicular lymphoma. J Clin Oncol 2003;21:3940–7.

43. Musolino A, Naldi N, Bortesi B, et al. Immunoglobulin G fragment C receptor polymorphisms and clinical efficacy of trastuzumab-based therapy in patients with HER-2/neu-positive metastatic breast cancer. J Clin Oncol 2008;26:1789–96.

44. Nimmerjahn F, Ravetch JV. Divergent immunoglobulin G subclass activity through selective Fc receptor binding. Science 2005;310:1510–2.

45. Treon SP, Hansen M, Branagan AR, et al. Polymorphisms in FcgRIIIA (CD16) receptor expression are associated with clinical response to rituximab in Waldenstrom's macroglobulinemia. J Clin Oncol 2005;23:474–81.

46. Hamaguchi Y, Xiu Y, Komura K, Nimmerjahn F, Tedder TF. Antibody isotype-specific engagement of Fcg receptors regulates B lymphocyte depletion during CD20 immunotherapy. J Exp Med 2006;203:743–53.

47. Uchida J, Hamaguchi Y, Oliver JA, et al. The innate mononuclear phagocyte network depletes B lymphocytes through Fc receptor-dependent mechanisms during anti-CD20 antibody immunotherapy. J Exp Med 2004;199:1659–69.

48. McEarchern JA, Oflazoglu E, Francisco L, et al. Engineered anti-CD70 antibody with multiple effector functions exhibits *in vitro* and *in vivo* antitumor activities. Blood 2007;109:1185–92.

49. Vervoordeldonk SF, Merle PA, van Leeuwen EF, van der Schoot CE, von dem Borne AE, Slaper-Cortenbach IC. Fc g receptor II (CD32) on malignant B cells influences modulation induced by anti-CD19 monoclonal antibody. Blood 1994;83:1632–9.

50. Cherukuri A, Cheng PC, Pierce SK. The role of the CD19/CD21 complex in B cell processing and presentation of complement-tagged antigens. J Immunol 2001;167:163–72.

51. Sieber T, Schoeler D, Ringel F, Pascu M, Schriever F. Selective internalization of monoclonal antibodies by B-cell chronic lymphocytic leukaemia cells. Br J Haematol 2003;121:458–61.